Automatic segmentation of contrast-enhanced time resolved image series[1]

Junhwan Kim[a] and Ramin Zabih[a,b,*]
[a]*Department of Computer Science, Cornell University, Ithaca, NY, USA*
[b]*Department of Radiology, Cornell University, Ithaca, NY, USA*

Abstract. Medical imaging often involves the injection of contrast agents and the subsequent analysis of tissue enhancement patterns. Many important types of tissue have characteristic enhancement patterns; for example, in MR mammography, malignancies exhibit a characteristic "wash out" temporal pattern, while in MR angiography, arteries, veins and parenchyma each have their own distinctive temporal signature. In such time resolved image series, there are substantial changes in intensities; however, this change is due primarily to the contrast agent, rather than to motion. As a result, the task of automatically segmenting contrast-enhanced images poses interesting new challenges.

In this paper, we propose a new image segmentation algorithm for time resolved image series with contrast enhancement, using a model-based time series analysis of individual pixels. We take an energy minimization approach to ensure spatial coherence. The energy is minimized in an expectation-maximization fashion that alternates between segmenting the image into a number of non-overlapping regions and finding the temporal profile parameters which describe the behavior of each region. Preliminary experiments on MR angiography and MR mammography studies show the algorithm's ability to find an accurate segmentation.

1. Introduction

Many medical imaging studies involve the injection of contrast agents, in order to visualize structures that cannot otherwise be segmented. The choice of the contrast medium depends upon the imaging modality; in CT, the contrast agents are iodine-based, while MR contrast agents use gadolinium [13]. In the resulting contrast-enhanced time resolved image series, the patient is often stationary, and the substantial changes in intensities that occur are due primarily to the contrast agent. Moreover, different types of tissues often have characteristic enhancement patterns, which form the basis for segmentation. This is especially true in MR; for example, in MR mammography, malignancies exhibit a characteristic "wash out"' temporal pattern, while in MR angiography, arteries, veins and parenchyma have distinct temporal profiles.

Automatic segmentation of contrast-enhanced time resolved image series poses novel challenges. At first glance, motion segmentation techniques such as [6,20] seem to be applicable. However, these methods are designed for situations where scene elements are moving with respect a conventional

---

*Corresponding author: Ramin Zabih, 4130 Upson Hall, Computer Science Dept., Ithaca, NY 14853-7501, USA. Tel.: +1 607 255 8413; Fax: +1 607 255 4428; E-mail: rdz@cs.cornell.edu.
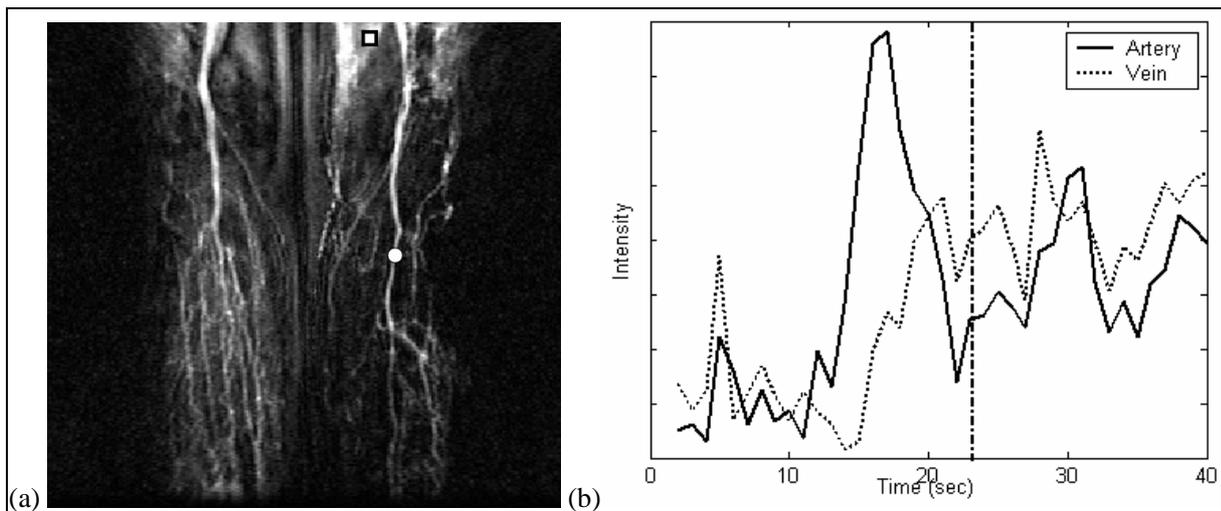
Fig. 1. (a) Snapshot from an MR angiography image sequence (b) Intensity profile of selected pixels.

camera. In medical imaging applications, the imaging devices are quite different from traditional cameras. Moreover, in contrast-enhanced time resolved image series it is common for the patient to be stationary. This is especially true for MR imaging, due to the well-known artifacts that motion produces in this imaging modality [13]. However, it is also often true in CT (for example, when imaging the brain) or lower abdomen. While there is obviously motion present (for example, at the cellular level) even in a stationary patient, the change in intensities observed in contrast-enhanced images is not due to the motion of scene elements.

In order to segment contrast-enhanced time resolved image series, it is vital to use the information in the sequence. There is simply not enough information in a single image to reliably perform segmentation. This can be easily seen from Fig. 1, which shows an example of contrast-enhanced MR angiography of the lower extremities. Figure 1(a) shows a snapshot from the image sequence (to make the arteries and veins visible, the image shown is the difference between a post-contrast image and a pre-contrast image). Figure 1(b) depicts the temporal (intensity) profiles of the selected pixels in Fig. 1(a). The dash-dot vertical line in Fig. 1(b) indicates where the snapshot in Fig. 1(a) is taken.

The circled pixel is on an artery, and its temporal profile shows a sharp increase when the contrast agent arrives. By comparison, the temporal profile of the vein pixel (indicated by the rectangle) shows a steady increase after the contrast agent arrives, which indicates that the blue pixel is on vein. However, the vein pixel is brighter than the artery pixel in the snapshot shown in Fig. 1(a), which would mislead an image segmentation method based on this snapshot image. An image segmentation algorithm based on the temporal profile of each pixel will have much higher chance to correctly classify these pixels as either artery or vein.

1.1. Overview of our approach

Our approach is based on the application of time series analysis to pixel temporal profiles. Time series analysis [8] is a set of techniques for analyzing a temporal series of observations. It has primarily been used in the financial community, for example to analyze commodity prices. However, the information contained in any individual pixel's temporal profile is noisy; in addition, a correct segmentation would
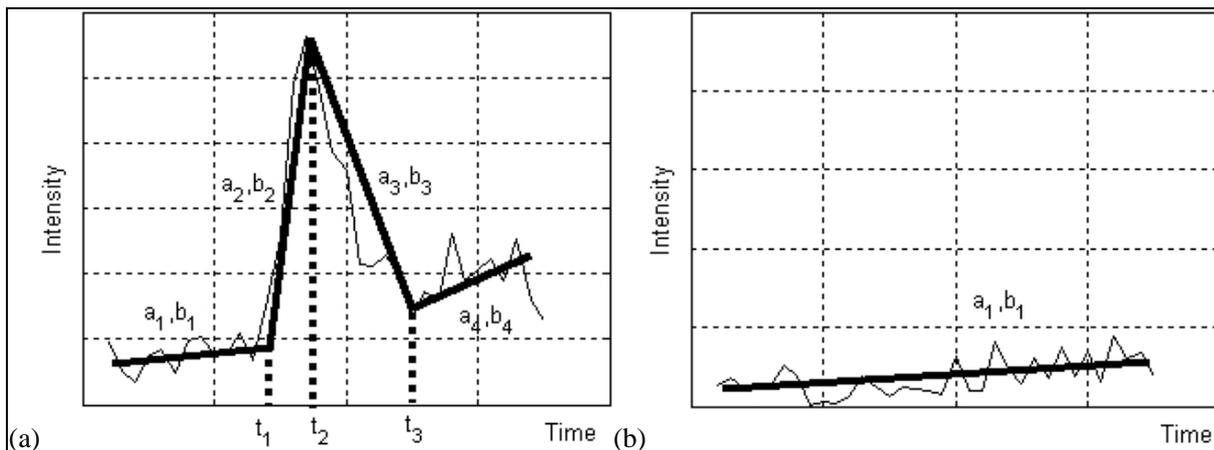
Fig. 2. Parameters for MR angiography image series (a) Artery (b) Vein/Parenchyma.

be spatially coherent (i.e., the pixels that should be labeled artery are not distributed independently at random through the image). This spatial coherence assumption allows us to overcome the noise in a single pixel's temporal profile.

We assume that for each type of tissue that is of interest, there is a model available of that tissue's temporal profile. For example, in MR angiography the model for an artery might be a peak formed by 4 line segments, while the model for a vein might be a gradual rise formed by 2 line segments (see Fig. 2). Eventually it might be possible to learn such a model from hand-labeled examples, but we currently assume that such a model already exists. Each model will have a number of parameters, which will need to be estimated. The input to our algorithm will be a set of models, together with an image sequence. The output will be a labeling of the pixels, such that each pixel is associated with a single model, together with an estimate for each model's parameters.

The algorithm itself is very similar in spirit to existing approaches to motion segmentation based on expectation-maximization [10] (we will describe some related work in the next section), and especially to [2]. We alternate between two steps. In the first step, given a set of models, each of which has some parameters, we must label each pixel with a model. In our method we follow the approach of [2] and use the graph cut algorithm of [7] to solve this problem. In the second step, we estimate the parameters for each model by analyzing the set of pixels that have been labeled with this model. Simple statistical techniques from time series analysis are used in both of these steps.

The rest of the paper is organized as follows. Section 2 summarizes related work. In Section 3, we give a formal definition of our problem. The two alternating steps of our algorithm are described in Section 4 and Section 5. Preliminary experimental results for MR angiography and MR mammography are given in Section 6. We conclude with some suggestions as to how our work can be extended to contrast-enhanced time resolved image series that also contain significant motion.

2. Related work

There is, of course, a great deal of prior work on image segmentation, primarily focusing on the segmentation of a single image. However, it does not appear that contrast-enhanced images can be segmented by looking at a single image; as a result, the most relevant related work involves segmentation of image series.

Several vision researchers have used time series analysis for various purposes [4,5,16,17], although they in general have not referred to these techniques by that name. Kanade et al. [14] built a VLSI sensor array for a rangefinder that gathers range data in parallel as a scene is swept continuously by a moving stripe. Each cell continuously records the time at which a peak is observed at each sensor pixel, and detects the time at which it observed the peak incident light intensity during the sweep of the stripe. Curless and Levoy [9] proposed a ranging method based on analyzing the time evolution of the structured light reflections. They use this information to correct systematic distortions of the range data that stem from curved surfaces, discontinuous surfaces, and surfaces of varying reflectance, thereby attaining significantly higher accuracy. Seitz and Dyer [18] provide another example of motion pattern analysis, by determining if an image sequence could have been produced by an object whose motion is periodic in some reference frame. Zhang et al. developed accurate shape acquisition systems using color structured light [22]. They solve the correspondence problem by using a multi-pass dynamic programming algorithm that eliminates the global smoothness assumptions and strict ordering constraints present in many formulations. Recently, they also proposed the "space-time stereo"' that recovers shapes by observing their appearance variations over time using a stereo pair [23]. They define the mean shape over a stereo pair of image series as the shape which has minimum matching error over space and time, and the shape variation is modeled as a stochastic linear dynamic system. The method is shown to generate better shape reconstruction than traditional stereo pair.

The body of work that is most closely related to ours is the research on expectation-maximization (EM) based segmentation of image series. Most of these methods deal with motion segmentation using layers [1,20,21]. The problem we address, however, is not motion segmentation, since there is no motion in the images. Moreover, these methods do not efficiently label pixels with the appropriate model while preserving spatial coherence. In order to do so, we use graph cuts. The basic technique is to construct a specialized graph for the energy function to be minimized, such that the minimum cut on the graph also minimizes the energy. Graph cuts have been successfully used for a wide variety of vision problems including image restoration, stereo motion, voxel occupancy, and medical imaging (see [7] for a more detailed discussion).

The closest work to ours is the algorithm of Birchfield and Tomasi [2], which is an EM-based method for stereo and motion with slanted surfaces that uses the graph cuts algorithm of [7] to label pixels. Their work, however, method does not analyze the temporal profile of individual pixels, and is not straightforwardly applicable to the task of segmenting contrast-enhanced time resolved image series.

3. Problem formulation

The input to our algorithm is a sequence of images $i : P \times T \to R$ for each pixel $p \in P$ and each time $t \in T = \{0, 1, 2, L, T - 1\}$ (see Fig. 5 for an example). For convenience, $i_p \in R^T$ denotes the temporal profile of the pixel p. We represent the output as a labeling $f : P \to L$, where L is the set of labels, along with temporal profile parameters θ_t for each label l. For instance, $L = \{$malignant tumor, benign tumor, non-tumor$\}$ for a breast image sequence, while $L = \{$artery, vein/parenchyma$\}$ for an MR angiography image sequence.[2] $\theta_t = \{a_l, b_l\}$ when the temporal profile is modeled by a straight line $i_{pt} = a_l t + b_l \cdot \theta_l$. will have more elements when we use more sophisticated models.

---

[2]The label vein/parenchyma will be used for veins as well as for parenchyma, which enhances similarly to veins. The portion of the image outside the patient's body can be easily detected automatically and not considered for further processing.

J. Kim and R. Zabih /   5

Our goal is to find a labeling that matches pixels of similar temporal profile while minimizing discontinuities. More specifically, we minimize the following energy functional:

$$E(f) = \sum_{p \in P} \sum_{q \in N_p} 2u_{pq}T[f_p \neq f_q] + \sum_{p \in P} g(i_p, p, \theta_{f_p}), \tag{1}$$

where the indicator functions $T[\cdot]$ is 1 if its argument is true and 0 otherwise. The first term enforces smoothness by penalizing the discontinuities. upq can be interpreted as a cost of a discontinuity between p and q [7]. The second term is a data-dependent energy term indicating the costs of assigning the labels to the pixel. $g(i_p, p, \theta_{f_p})$ is the cost of assigning the label f_p to the pixel p whose temporal profile is i_p.

To minimize the energy functional, we alternate between segmenting the image into disjoint regions by assigning a label to every pixel and finding the temporal profile parameters of each region. We will describe these two steps in the next two sections.

4. Assigning labels to pixels

Once the temporal profile parameters for each region are available, we can assign the labels to pixels by calculating the residuals followed by an optimization. First, we calculate the residuals for each pixel to each label:

$$r_{pl} = r(i_p, \theta_{f_p}) \tag{2}$$

The way we evaluate the residual hinges on how we model the temporal profile.

MR ANGIOGRAPHY: Figure 2 depicts the parameters for each label in MR angiography image series. Note that the parameter set θ_l can be different depending on label l. The temporal profile for artery pixels is modeled by 4 line segments. Thus we have 8 parameters (a'_{iA}s and b'_{iA}s) for each line segment and 3 parameters ($t_{iA'}$s) for the intersection of consecutive line segments, which leads to $\theta_{\text{Artert}} = \{a_{1A}, b_{1A}, t_{1A}, a_{2A}, b_{2A}, t_{2A}, a_{3A}, b_{3A}, t_{3A}, a_{4A}, b_{4A}\}$. Similarly, we have $\theta_{\text{Vein/Parenchyma}} = \{a_{1V}, b_{1V}, t_{1V}, a_{2V}, b_{2V}\}$. The temporal profile of the region whose label is l and whose model is parameterized by n line segments is given by

$$j_{it} = \begin{cases} a_{1l}t + b_{1l} \text{ if} & t < t_1 \\ a_{1l} + b_{1l} \text{ if } t_{k-1} \leqslant t < t_k, (2 \leqslant k \leqslant n-1) \\ a_{1l}t + b_{1l} \text{ if} & t_{n-1} \leqslant t \end{cases}$$

MR MAMMOGRAPHY: According to recent findings [11,19], malignant lesions are characterized in MR imagery by rapid wash-in and rapid wash-out. On the other hand, benign lesions are characterized by rapid wash-in and slow wash-out (see Fig. 3). To capture these properties, we model the temporal profile of lesion by two line segments, i.e., one for wash-in and the other for wash-out ($\theta_{\text{Malignant-lesion}} = \{a_{1M}, b_{1M}, t_{1M}, a_{2M}, b_{2M}\}$, $\theta_{\text{Benign-lesion}} = \{a_{1B}, b_{1B}, t_{1B}, a_{2B}, b_{2B}\}$). For non-lesions, we use one line as a model of the temporal profile ($\theta_{\text{Non-lesion}} = \{a_{1N}, b_{1N}\}$) (see Fig. 4).

Once we have the model of the temporal profile, the residual for assigning the label l to the pixel p to is given by

$$r(i_p, \theta_l) = \min_{\beta_p \Delta t_p} \frac{1}{N} \sum_{t_{\text{Min}} \leqslant t \leqslant t_{\text{Max}}} \rho(i_{pt}, \beta_p j_{p(t+\Delta t_p)}),$$
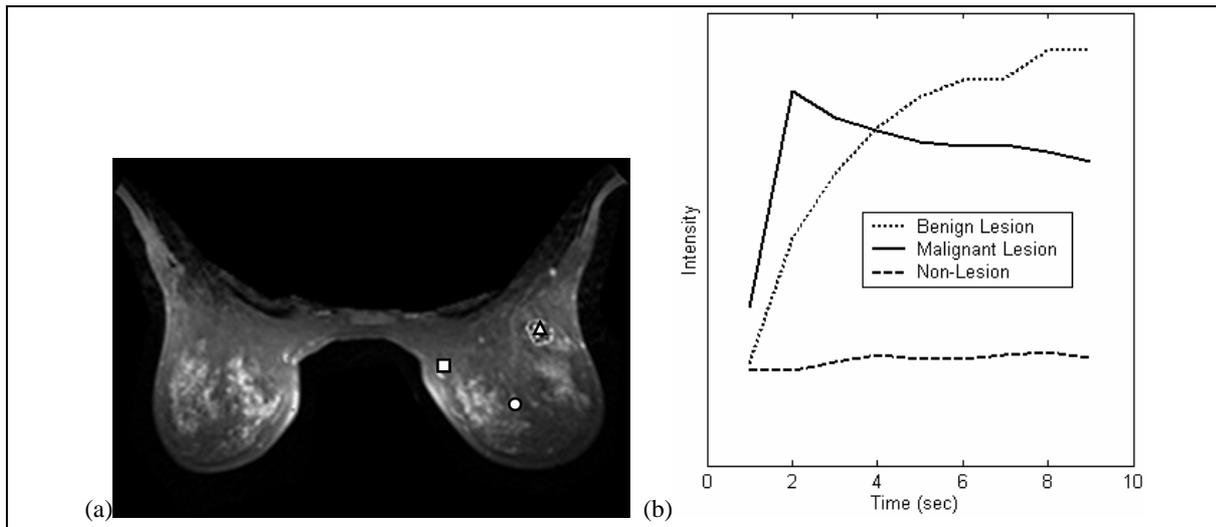
Fig. 3. (a) A snapshot of a mammography image sequence (b) Temporal profile of the selected pixels.
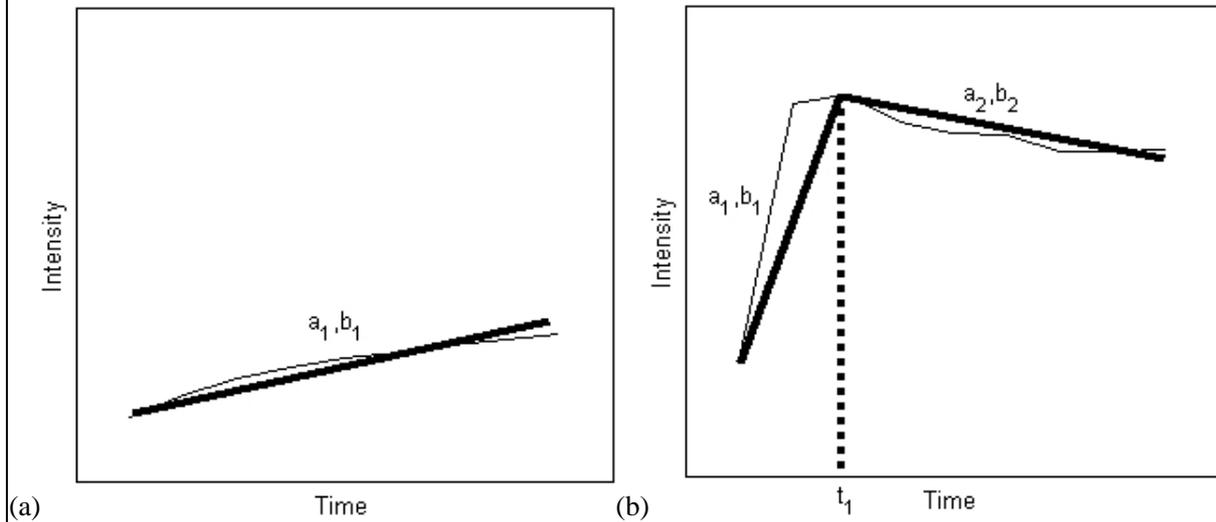

Fig. 4. Parameters for MR angiography image series (a) Lesion (b) Non-Lesion.

where $t_{\mathrm{Min}} = \max(0, -\Delta t_p)$, $t_{\mathrm{Max}} = \min(T, T - \Delta t_p) - 1$, and $\frac{1}{N}$ is the normalization constant, or $N = t_{\mathrm{Max}} - t_{\mathrm{Min}} + 1$. Also, Δt_p and β_p are the time displacement and intensity scale of pixel p. We introduced Δt_p and β_p to offset the variation on time displacement and intensity scale between pixels. For the distance metric ρ, we use $\rho = \min(|x - y|, K)$ for some constant K following Eq. (3). Based on the residual, we calculate the cost of assigning the labels to each pixel:

$$g(i_p, p, \theta_{f_p}) = \frac{\exp(-r_{pl}^2/2\sigma^2)}{\sum_{l' \in L} \exp(-r_{pl'}^2/2\sigma^2)}, \tag{3}$$

where σ corresponds to the amount of residual expected in the data. To find an approximate solution to this problem, we use the expansion move algorithm of [7]. Since minimizing Eq. (1) has been shown

to be NP-hard [7], the algorithm is not guaranteed to find the global minimum. Nevertheless, it finds a good local minimum, in the sense that the final energy cannot be reduced by increasing the set of pixels having a single common label. After the graph cut algorithm has converged, we find the temporal profile parameter for each label, as explained in the next section.

5. Estimating temporal profile parameters

The temporal profile parameters of each label describe how the pixel intensity of a pixel with the label will vary over time. Once the assignment of labels to each pixel is known, we can find the average temporal profile of all the pixels in each label. Simply put,

$$\theta_l = \text{ExtractParameters} \left(\sum_{p \in P, f_p = l} = l \beta_p i_{p(t + \Delta t_p)} \right), \tag{4}$$

where Δt_p and β_p are time displacement and intensity scale of pixel p. Again, $ExtractParameters$ depends how we model the temporal profile.

MR ANGIOGRAPHY: To estimate the parameters, we first estimate the intersection times (t'_{il}s), then estimate the line segment coefficients (a'_{iA}s and b'_{iA}s) between the intersection times by using the least square fitting. More specifically, for the parameters for artery, t_{1A} is the first time index such that intensity at t_{1A} is above $\mu + k\sigma$, where μ and σ are the mean and the standard deviation of the intensities for the time index from 1 to $t_{1A} - 1$. We set $k = 2.5$ in our experiments. t_{3A} is estimated similarly except we examine whether the intensity is above going backwards. t_{2A} is set to be the time index that has the maximum intensity between t_{1A} and t_{3A}. For the parameters for veins/parenchyma, t_{1V} is the time index that has the minimum intensity in a predefined range. Since we have only two labels, we don't actually have to use the graph cut algorithm of [7], but we can use the 2-way cut algorithm from [12], which gives the global optimal labeling in polynomial time.

MR MAMMOGRAPHY: Similar to the case of MR angiography data, we use robust least square fitting to extract parameters for the non-lesion label. We set t_1 to be the time index that has the maximum intensity in a predefined range, namely 2 to 4, since it is known that the wash-in and wash-out phases intersect between times 2 and 4 [11,19].

6. Experiments

In this section, we give some experimental results on MR angiography data and mammography data that use our algorithm. In each experiment, we show how we obtain the data, how to model temporal profiles, how to extract temporal profile parameters, and result of our algorithm.

6.1. Trifurcation

Contrast enhanced magnetic resonance angiography (CEMRA) has become a routine clinical tool for pre-treatment mapping of vasculature [15]. Figure 5 shows an example of MR angiography data, which typically consists of 30 to 40 images.

It is difficult to compare our results with previous work, since to our knowledge no other methods have been published for segmenting contrast-enhanced time resolved image series. However, there is a
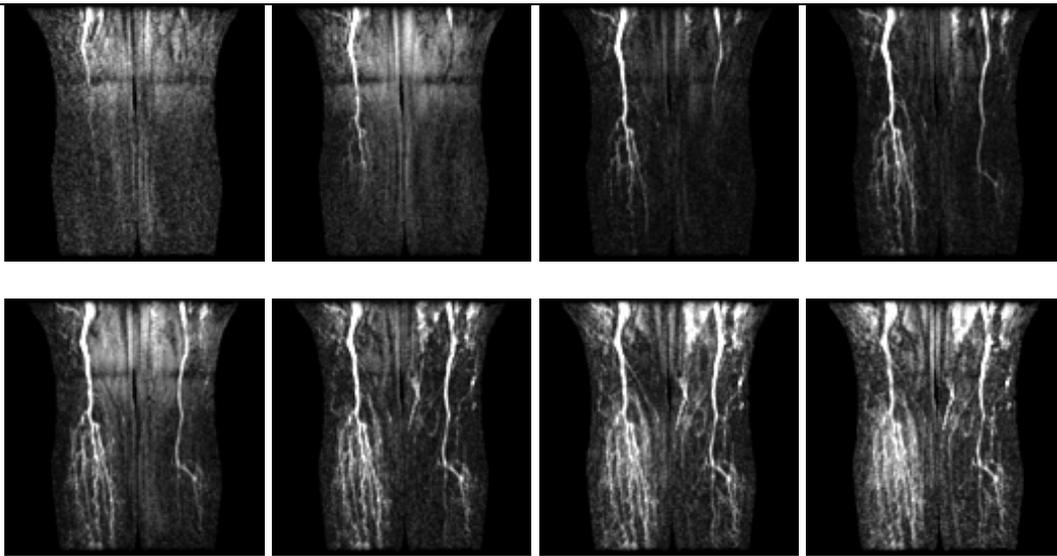
Fig. 5. An MR angiography image series, read from top to bottom and left to right.

comparison that we find instructive, in that it shows the importance of doing segmentation based on the temporal pixel histories in the entire image sequence, rather than on a single image. We obtained several series where an experienced radiologist hand-selected a pair of images (pre-contrast and post-contrast), such that the difference image gave the clearest view of the arteries. This manually selected difference image can then be compared to the result of our algorithm. These results are shown in the left and middle columns of Fig. 6. Visual inspection clearly shows that our algorithm gives far less false artery (i.e. a vein/parenchyma pixel misclassified as an artery), which mainly results from movement of patient, and far less false vein/parenchyma (i.e. an artery pixel misclassified as a vein/parenchyma), which primarily comes from faint signal because of bad timing. Both of these advantages come from our algorithm's use of the entire image sequence.

In Fig. 6 we have also added an additional comparison in the rightmost column. Here we have applied a binary segmentation algorithm to the hand-generated image in the leftmost column. Since spatial coherence is very important, instead of a simple threshold scheme we used a simple algorithm based on graph cuts that finds connected groups of bright pixels. We believe that the poor results obtained by this method demonstrate the importance of using the entire image sequence, rather than doing static segmentation on a single image.

6.2. *Mammography*

In MR mammography, a series of 9 images are taken approximately 90 seconds apart, and the contrast agent is injected immediately after the first image acquisition. Figure 7 shows the result of image segmentation overlaid with one input image at a specific time. Currently, we use the second image. Body parts other than breast are removed manually to simplify the parameter estimation process, although it should be relatively easy to automate this removal process given that the image orientation is fixed. The results show that our algorithm avoids being distracted by very bright pixels that occur mainly on veins. Any image segmentation algorithm based on one single image will have no clue to distinguish such pixels from lesion pixels. In these two cases, an experienced radiologist who did not
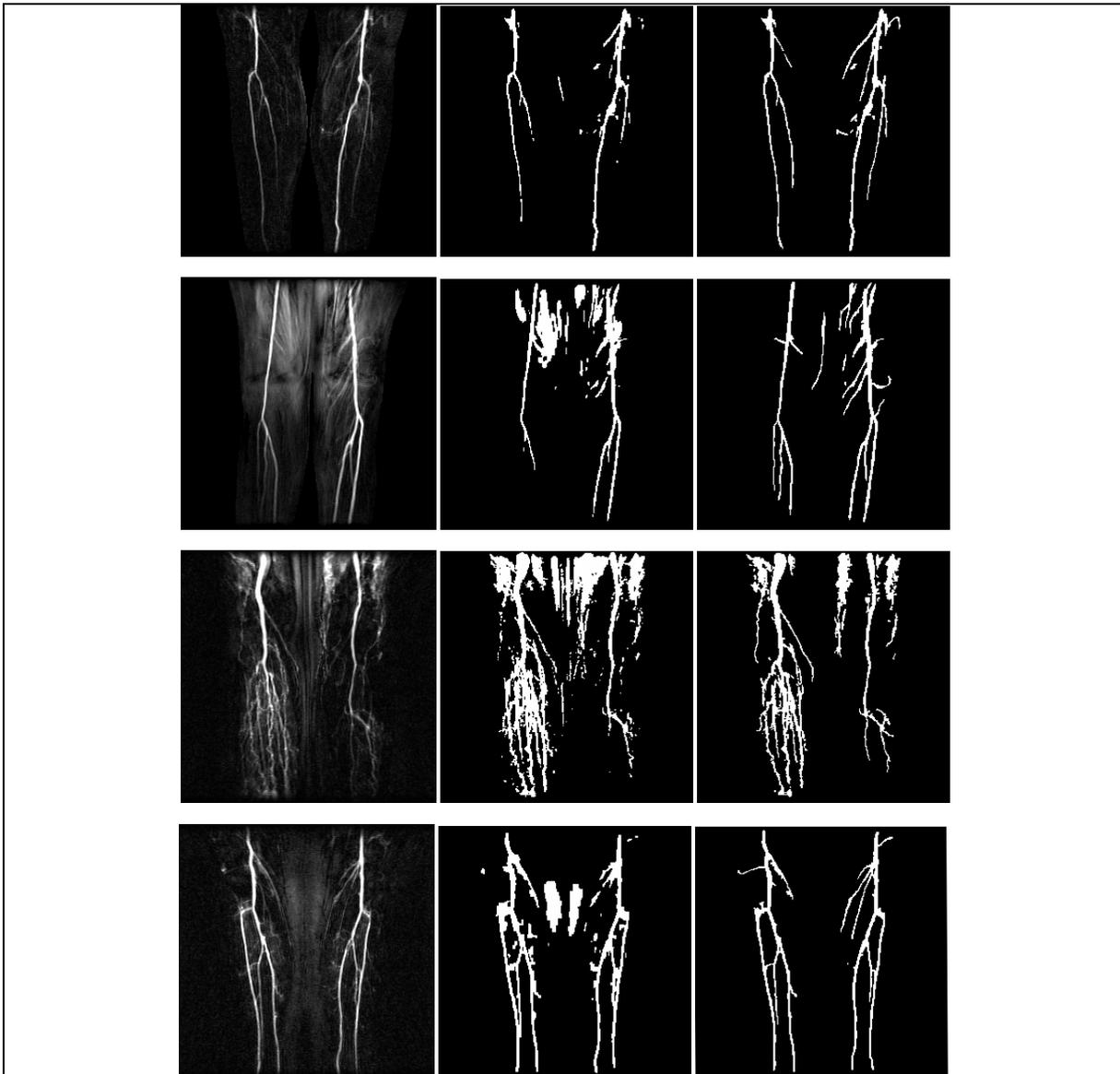
Fig. 6. Left: Best difference image manually selected by an experienced radiologist. Middle: Results from our algorithm. Right: Results from segmentation of the manually selected difference image.

use our system believed that the patient had malignancies in approximately the region detected by our method; this diagnosis was confirmed by biopsy.

7. Extensions

The methods that we have described show promising preliminary results for MR angiography and MR mammography. However, there are a number of ways in which these results could be improved.
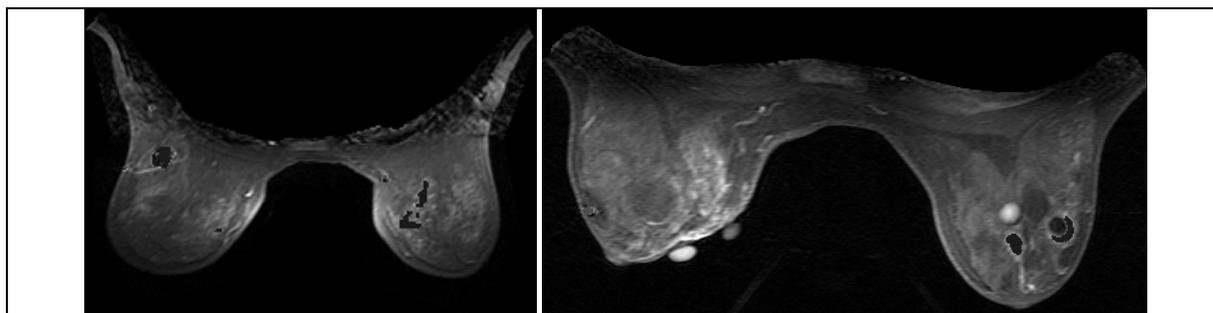
Fig. 7. Results of our algorithm. Malignant lesion (in red) and benign lesion (in blue) are overlaid with an input image at time index $= 2$.

For example, the temporal models that we have used in our experiments to date are fairly simple. It is important to note that our algorithm does not require a particular temporal model for pixel behavior, as long as there is some piecewise model where we can pre-specify the number of pieces. There is no restriction that the pieces need to be linear, although piecewise linear models like the ones we have used are obviously the first class that should be explored. It would be interesting to apply more sophisticated temporal models for these problems, such as autoregressive models or pharmacologically derived models. In addition, the experimental results we have described are quite preliminary, and a more careful comparison with the results of other segmentation algorithms should be performed, ideally using some kind of (probably hand-segmented) data as the gold standard.

Our preliminary experiments show promising results for contrast-enhanced image sequences, such as MR angiography and MR mammography, where the patient is usually stationary. However, it would be interesting to extend our approach to image sequences with both contrast and motion, e.g., coronary artery images where the heart is clearly visible and beating as the contrast flows in and out. Currently, our technique is based on the assumption that there is no motion, i.e., each time series stems from same pixel. Of course, if we know exactly how each pixel moves, we still can obtain the time series from same pixel. It may be possible to handle unknown motions by do the same calculation based on an assumption about the motion of each pixel, and then re-estimating the motion. In other words, instead of iterating between pixel labeling and parameter estimation, we can iterate between pixel labeling, parameter estimation, and motion estimation. Of course, the more compactly we can represent the motion (i.e., fewer motion parameter we have), the more likely it is that this algorithm converges to the desired solution.

References

[1] Serge Ayer and Harpreet Sawhney, *Layered representation of motion video using robust maximum-likelihood estimation of mixture models and MDL encoding*, In International Conference on Computer Vision, 1995, pp. 777–784.
[2] S. Birch.eld and C. Tomasi, *Multiway cut for stereo and motion with slanted surfaces*, in International Conference on Computer Vision, 1999, pp. 489–495.
[3] M. Black and P. Anandan, The robust estimation of multiple motions: Parametric and piecewise-smooth flow fields, *Computer Vision and Image Understanding* **63**(1) (Jan. 1996), 75–104.
[4] A.F. Bobick and J.W. Davis, The recognition of human movement using temporal templates, *IEEE Transactions on Pattern Analysis and Machine Intelligence* **23**(3) (March, 2001), 257–267.
[5] Jean-Yves Bouguet and Pietro Perona, *3D photography on your desk*, in International Conference on Computer Vision, 1998, pp. 43–52.
[6] Patrick Bouthemy and Edouard Francois, Motion segmentation and qualitative dynamic scene analysis from an image sequence, *International Journal of Computer Vision* **10**(2) (April, 1993), 157–182.

[7]   Yuri Boykov, Olga Veksler and Ramin Zabih, Fast approximate energy minimization via graph cuts, *IEEE Transactions on Pattern Analysis and Machine Intelligence* **23**(11) (November, 2001), 1222–1239.

[8]   J Cromwell, W. Labys and M. Terraza, *Univariate Tests for Time Series Models*, Sage Pub, 1994.

[9]   Brian Curless and Marc Levoy, *Better optical triangulation through space-time analysis*, in International Conference on Computer Vision, 1995, pp. 987–994.

[10]   A. Dempster, N. Laird and D. Rubin, Maximum likelihood from incomplete data using the EM algorithm, *Journal of the Royal Statistical Society, Series B* **39** (1977), 1–38.

[11]   G.P. Liney, P. Gibbs, C. Hayes, M.O. Leach and L.W. Turnbull, Dynamic contrast-enhanced MRI in the differentiation of breast tumors: user-defined versus semi automated region-of-interest analysis, *Magnetic Resonance Imaging* **10**(6) (1999), 945–949.

[12]   D. Greig, B. Porteous and A. Seheult, Exact maximum a posteriori estimation for binary images, *Journal of the Royal Statistical Society, Series B* **51**(2) (1989), 271–279.

[13]   H. John Juhl, B. Andrew, Crummy and E. Janet, *Kuhlman. Paul and Juhl's Essentials of Radiologic Imaging*, Lippincott Williams & Wilkins, 1998.

[14]   T. Kanade, A. Gruss and L. Carley, *A very fast VLSI range finder*, in IEEE International Conference on Robotics and Automation, 1991, pp. 1322–1329.

[15]   M.R. Prince, T.M. Grist and J.F. Debatin, *3D Contrast MR Angiography*, Springer-Verlag, New York, 1998.

[16]   Kari Pulli, Habib Abi-Rached, Tom Duchamp, Linda G. Shapiro and Werner Stuetzle, *Acquisition and visualization of colored 3D objects*, in International Conference on Pattern Recognition, 1998, pp. 11–15.

[17]   P. Saisan, G. Doretto, Y. Wu and S. Soatto, *Dynamic texture recognition*, In IEEE Conference on Computer Vision and Pattern Recognition, 2001, pp. 58–63.

[18]   S.M. Seitz and C.R. Dyer, View-invariant analysis of cyclic motion, *International Journal of Computer Vision* **25**(3) (1997), 231–251.

[19]   S. Sinha, F.A. Lucas-Quesada, N.D. DeBruhl, J. Sayre, D. Farria, D.P. Gorczyca and W. Bassett, Multifeature analysis of Gd-enhanced MR images of breast lesions, *Journal of Magnetic Resonance Imaging* **7** (1997), 1016–1026.

[20]   John Wang and Edward Adelson, Representing moving images with layers, *IEEE Transactions on Image Processing* **3**(5) (September, 1994), 625–638.

[21]   Y. Weiss and E.H. Adelson, *A unified mixture framework for motion segmentation: Incorporating spatial coherence and estimating the number of models*, in IEEE Conference on Computer Vision and Pattern Recognition, 1996, pp. 321–326.

[22]   Li Zhang, Brian Curless and Steven M. Seitz, *Rapid shape acquisition using color structured light and multi-pass dynamic programming*, in 1st international symposium on 3D data processing, visualization, and transmission, 2002, pp. 19–21.

[23]   Li Zhang, Brian Curless and Steven M. Seitz, *Space-time stereo*, Submitted for publication, 2003.